STRATEGIES FOR DETECTION OF FLOODPLAIN INUNDATION WITH MULTI-FREQUENCY POLARIMETRIC SAR

Laura L. Hess* and John M. Melack**

*Dept. of Geography and **Dept. of Biological Sciences
University of California, Santa Barbara, CA 93106

Introduction

Mapping of floodplain inundation patterns is a key element in developing hydrological and biogeochemical models for large tropical river basins such as the Amazon. Knowledge of the time sequence of inundation is necessary to determine both water routing and biogenic gas fluxes (Richey et al. 1990). SAR is uniquely suited for this application because of its ability to penetrate cloud cover and, in many cases, to detect flooding beneath a forest or herbaceous canopy (Hess et al. 1990). We are currently developing a procedure for discriminating flooded forest, flooded herbaceous vegetation, and open water from other cover types for a coastal wetland site on the lower Altamaha floodplain, Georgia, emphasizing robust classifiers that are not site-specific.

Study site and methods

Multiple datatakes over a range of incidence angles were obtained for the Altamaha site by the JPL polarimetric SAR in March 1990 and again in May 1991. For both dates, the Altamaha was at high flood stage, and the entire floodplain other than sand ridges was inundated. Water levels were documented by extensive ground observations during the overflight. A rich variety of wetland types occur in the study site, including cypress-tupelo swamp *(Taxodium distichum, Nyssa aquatica)*, bottomland hardwood forest *(Nyssa* spp., *Taxodium distichum, Fraxinus* spp., *Acer rubrum, Liquidambar styraciflua)*, and marshes dominated by *Spartina alterniflora, Juncus roemerianus*, and *Zizaniopsis miliacea*. Upland sites are predominantly loblolly pine *(Pinus taeda)* plantations. Results given in this summary are for a March 1990 scene calibrated with JPL's SUPERCAL software using corner reflectors. The radar variables used in the analysis are HH, VV, and HV radar cross-sections per unit area (σ^0) and HH-VV phase difference for C, L, and P-bands, and ratios directly derived from these parameters. A 5X5 median filter was applied to the radar cross-sections to reduce within-class variability. Initial analysis was performed on 100 pixels in each of five cover types: open water, clearing, marsh, pine, and flooded forest. For each category, five 20-pixel windows were selected, representing a range of incidence angles and vegetation variability within each category. Because nearly all hardwood forests in the scene were flooded at the time of the overflight, pine forests are used to represent unflooded forests.

Discrimination of cover types

Discussion in this summary will be limited to two of the radar parameters found to be the most useful: PHH to CHH ratio and L-band phase difference. In Figure 1, σ^0_{PHH} is plotted vs. σ^0_{CHH} for unfiltered and median-filtered data; each plotted character represents a pixel. Separation between the classes is good, though not absolute, for the filtered data; overlap in the unfiltered data makes discrimination impossible. For the filtered data, mean σ^0 values for flooded forest and pine respectively are -8.2 dB and -12.8 dB at CHH and -1.1 dB and -4.6 dB at PHH. Although the means are distinct at both bands, there is enough spread in the data to cause confusion between the pine and

flooded forest categories.

Figure 2 demonstrates the behavior of phase difference at L band and C band for flooded forest. These phase difference histograms are presented on a circular scale rather than the usual linear one. There is a distinct shift toward phase differences close to 180° for flooded forests at L band, indicative of double-bounce scattering; this is not the case for pines. However, the phase difference distribution is too broad to perform well as a classifier, and phase difference, because of its circular nature, does not lend itself to techniques such as median filtering. We have found that by classifying the phase difference into one of three types and then applying a modal filter, confusion between pines and flooded forests is largely eliminated. Phase differences from 0°-70° or 270°-360° are classed as type 1, those centered on 180° (110°-250°) are considered type 3, and intermediate phase differences (70°-110° or 250°-290°) are type 2. A 3X3 pixel modal filter is then applied to the data, creating regions of uniform phase difference type. Although this technique is conceptually very simple, results to date show excellent separation between flooded forest and other categories. Table 1 shows the number of pixels classified in each type for 1000 pixels each from the marsh, pine, and flooded forest categories. Ninety-nine percent of the flooded forest pixels were classed as type 3. Only 1 non-flooded-forest pixel was type 3, and six flooded forest pixels were type 2.

Table 1. LHH-LVV phase difference types for 1000-pixel samples of marsh, pine, and flooded forest

	Type 1	Type 2	Type 3
Marsh	520	479	1
Pine	970	30	0
Flooded forest	0	6	994

The scatter plot for filtered σ^0_{PHH} vs. σ^0_{CHH} suggests that, following widely used parametric classification procedures, combinations of parameters could be found to provide a highly accurate separation between the cover types. The classification procedure would be tailored to the radar signatures (means and covariance matrices) for that particular scene. The limitation of this approach is that good results usually would not be obtained when applying the signatures to other scenes. Even for the same scene, signatures will vary temporally due to seasonal changes in scene properties such as leaf area index. Because we plan to apply this procedure to a broad spatial and temporal domain, scene-by-scene optimization of parametric classifiers is impractical. A knowledge-based approach using convergent evidence (Wharton 1989) seems best suited to this task.

Acknowledgements

This work is funded by the NASA SIR-C/XSAR program, JPL contract #958469.

References

Hess, L.L., J.M. Melack, and D.S. Simonett, 1990, Radar detection of flooding beneath the forest canopy: a review. *Int. J. of Remote Sensing* 11(7): 1313-1325.

Richey, J.E., J.B. Adams, and R.L. Victoria, 1990, Synoptic-scale hydrological and biogeochemical cycles in the Amazon River basin: a modeling and remote sensing perspective. In R.J. Hobbs & H.A. Mooney, eds., *Remote sensing of biosphere functioning*. New York: Springer-Verlag.

Wharton, S.W., 1989, Knowlege-based spectral classification of remotely sensed image data. In G. Asrar, ed., *Theory and applications of optical remote sensing*. New York: John Wiley & Sons.

Fig. 1a. Unfiltered data, Clearing (C), Marsh (M), Pine (P), Flooded Forest (F)

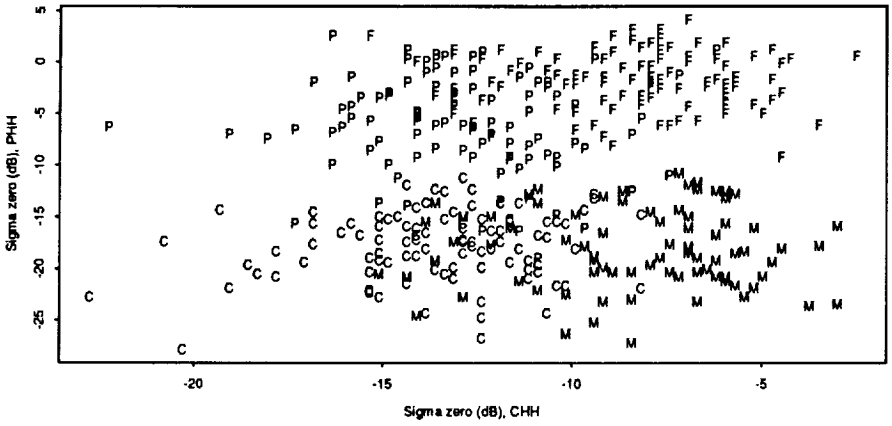

Fig. 1b. Filtered data, Clearing (C), Marsh (M), Pine (P), Flooded Forest (F)

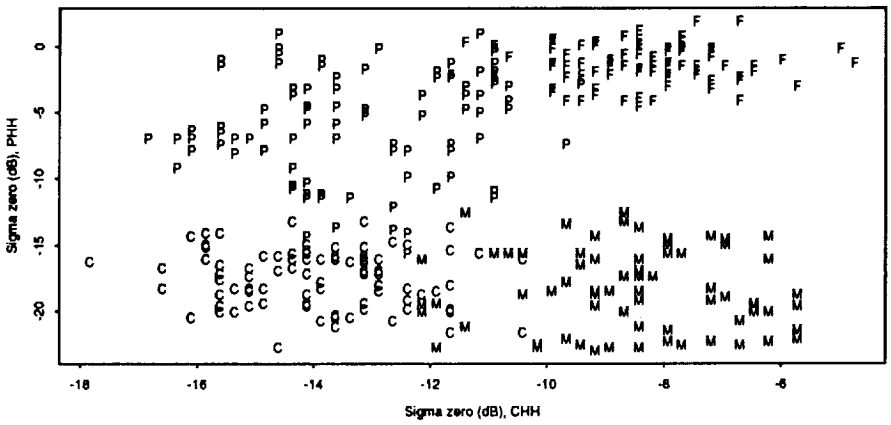

Fig. 2a. HH-VV phase difference

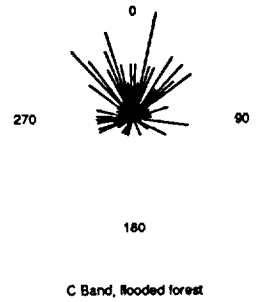

Fig. 2b. HH-VV phase difference